Mutual Information Statistics and Beamforming Performance Analysis of Optimized LoS MIMO Systems

Michail Matthaiou, *Member, IEEE,* Paul de Kerret, *Student Member, IEEE,*
George K. Karagiannidis, *Senior Member, IEEE,* and Josef A. Nossek, *Fellow, IEEE*

***Abstract*—This paper provides a systematic mutual information (MI) and multichannel beamforming (MBF) characterization of optimized multiple-input multiple-output (MIMO) communication systems operating in Ricean fading. These optimized configurations are of high practical importance since, contrary to the common belief, benefit from the presence of direct Line-of-Sight (LoS) components and deliver maximum multiplexing gains, by deploying specifically designed antenna arrays at both ends. In the following, using elements from random matrix theory, novel analytical expressions are derived for the exact and asymptotic MI statistics while the prevalent Gaussian approximation is examined. Moreover, new explicit expressions for the marginal eigenvalues are deduced which are thereafter used to analyze the BF performance of the associated eigenmodes in terms of Signal-to-Noise ratio (SNR) outage probability. We note that all derived formulas are given in tractable determinant form and therefore allow for fast and efficient computation and also yield an excellent match with Monte-Carlo simulations, under different fading scenarios and model parameters.**

***Index Terms*—Mutual information, MIMO systems, Ricean fading, Wishart matrices, eigenvalue distributions.**

I. Introduction

THE rapid development of multiple-input multiple-output (MIMO) systems over the past decade, has been mainly based on the grounds of Rayleigh fading (either independent and identically distributed (i.i.d.) or correlated), where no Line-of-Sight (LoS) path is present and a high number of multipath components is created by the surrounding environment [1]–[5]. Although the assumption of Rayleigh fading simplifies extensively the performance analysis of MIMO systems, its validity is often violated due to either a specular wavefront or a strong direct component; then, the entries of the channel matrix can be more effectively modeled via the Ricean distribution. Conceptually, LoS propagation is viewed to limit MIMO advantages because the channel matrix is normally rank deficient due to the linear dependence of the LoS rays' phases [6]–[8]. This makes the differentiation of the received signals at the MIMO detector laborious, thereby causing a high percentage of erroneously detected transmitted signals.

Some recent investigations though have questioned this belief and proposed design methodologies in order to achieve subchannel orthogonality which is a key condition for capacity maximization [9]–[13]. The common idea behind all these approaches is to place the antenna elements sufficiently far apart so that the spatial LoS responses become unique with a phase difference of $\pi/2$. The optimum spacings can be easily worked out via simple geometrical tools, while the mean channel matrix becomes full-rank and delivers equal LoS eigenvalues. Henceforth, we will refer to these configurations as *optimized LoS MIMO systems*. The fundamental feature of these configurations is that they yield maximal capacity at any given Ricean K-factor, under uniform power allocation (UPA) [9], [10], [12], [13]. As such, their mean MI (ergodic capacity) can be used to evaluate the difference between the theoretical capacity and the rate achieved in practice.

In the context of MIMO Ricean channels, we first note the work in [6] in which exact expressions for the mutual information (MI) statistics were derived; yet, the final results were given in integral form containing hypergeometric functions and therefore can be evaluated only numerically. In [14], the exact ergodic capacity was investigated when the transmitter (Tx) has full channel state information (CSI) while in [7] the authors derive asymptotic expressions for the mean MI when the Signal-to-Noise ratio (SNR) goes to infinity and the average channel matrix is rank-1. In [15], the MI higher-order statistics were derived in integral form using the joint (un)-ordered eigenvalue distributions. A plethora of recent works focused on MIMO capacity bounds for the case of Ricean fading. The most general approach so far has been reported in [16] which deduced several upper/lower capacity bounds assuming all different types of spatial correlation. We also recall the alternative approaches of [8], [17]–[19] which provide useful insights into this interesting area. In [20], some simplified expressions for the elementary functions of Wishart matrices were given which were thereafter used to upper and

Paper approved by N. Al-Dhahir, the Editor for Space-Time, OFDM and Equalization of the IEEE Communications Society. Manuscript received December, 16, 2009; revised April 6, 2010 and June 10, 2010.

Part of this paper was presented at the IEEE International Conference on Communications (ICC), Cape Town, South Africa, May 2010.

M. Matthaiou was with TU München, Germany. He is now with the Department of Signals and Systems, Chalmers University of Technology, SE-412 96, Gothenburg, Sweden (e-mail: michail.matthaiou@chalmers.se).

P. de Kerret is with the Institute for Theoretical Information Technology, RWTH Aachen University, Sommerfeldstrasse 24, 52074, Aachen, Germany (e-mail: dekerret@ti.rwth-aachen.de).

G. K. Karagiannidis is with the Department of Electrical and Computer Engineering, Aristotle University of Thessaloniki, 54 124, Thessaloniki, Greece (e-mail: geokarag@auth.gr).

J. A. Nossek is with the Institute for Circuit Theory and Signal Processing, Technische Universität München (TUM), Arcistrasse 21, 80333, Munich, Germany (e-mail: nossek@nws.ei.tum.de).

Digital Object Identifier 10.1109/TCOMM.2010.091710.090770

lower bound the MI complementary cumulative distribution function (CDF). Finally, the seminal work of [21] considered the asymptotic MI statistics of doubly-correlated LoS MIMO systems using the replica method. The common characteristic of the above mentioned papers is that they consider either the tractable case of rank-1 systems [6]–[8], [15], [17], [18] or the case of distinct LoS eigenvalues [15]–[17].

Apart from capacity statistics, a critical issue is the design of optimal linear transceivers (linear precoder/equalizer) for enhancing the performance of multichannel beamforming (MBF) MIMO systems, and consequently, minimize the error rates. When perfect CSI is available at both the Tx and receiver (Rx), the optimum strategy is to convey data streams across the channel eigenmodes, or the orthogonal spatial subchannels that are established in a typical MIMO link. A comprehensive theoretical framework for this choice was given in [22], and since then has been widely used in the corresponding literature [23]–[25]. In order to analytically characterize these systems in terms of outage probability, we have to obtain explicit expressions for the marginal eigenvalue distributions. In this context, a generic analytic framework for the marginal eigenvalue distributions of different classes of Wishart matrices (both central and noncentral), can be found in [26]–[28]. For the specific case of Ricean fading, a similar analysis was performed in [25] for arbitrary rank of the mean channel matrix but with distinct eigenvalues.

To the best of the authors' knowledge, little is still known for the capacity statistics and MBF performance of optimized LoS MIMO configurations. This can be partially attributed to the difficulty in manipulating complex non-central Wishart matrices in this limiting case. While the authors in [9]–[12] propose tractable design methodologies for maximizing LoS MIMO capacity, no statistical characterization is being performed. Only recently, the MI probability density function (PDF) was deduced but this analysis was tied to dual configurations where the minimum number of antennas is two [29].

The main paper contributions can now be summarized as:

- We first extend the results of [6] to account for the case of orthogonal LoS subchannels with identical eigenvalues. In order to tackle the determinant limits of type $0/0$ that appear throughout, we invoke a useful technique proposed recently in [30] that lends itself into tractable manipulations. Novel explicit expressions, that are analytically friendlier and more insightful than the ones of [6], are presented for the exact MI mean and variance of optimized LoS MIMO systems, via its moment generating function (MGF); these expressions apply for an *arbitrary number* of antenna elements. In the high-SNR regime, we provide tractable formulas for the MI statistics, via the generalized variance of the MIMO correlation matrix, that reveal interesting implications of the model parameters on MIMO capacity. We also explore the Gaussianity approximation for the MI distribution with our numerical results indicating that it is valid under different fading scenarios.
- In the second part, we capitalize on the works of [23]–[25] to provide a thorough MBF performance analysis. New explicit formulas for the ordered marginal/unordered CDF/PDF eigenvalue distributions are derived, in order to assess the SNR statistics of the associated eigenmodes. Moreover, first-order expansions for the marginal eigenvalue distributions are given, and applied to the asymptotic outage characterization.

The rest of the paper is organized as: In Section II, the MIMO channel model is introduced along with the limiting joint eigenvalue PDF. In Section III, we deduce analytical expressions for the exact/asymptotic MI statistics and introduce the Gaussianity approximation. The MBF performance is assessed in Section IV. A set of numerical results is given in Section V. Finally, Section VI concludes the paper.

Notation: We use upper and lower case boldface to denote matrices and vectors, respectively. The (i,j)-th entry of an $m \times n$ matrix $\mathbf{X}$ is $\{\mathbf{X}\}_{i,j}$ with $1 \leq i \leq m$ and $1 \leq j \leq n$. An $n \times n$ identity matrix is expressed as $\mathbf{I}_n$. The symbols $(\bullet)^T$, $(\bullet)^\dagger$ represent the transpose and Hermitian transpose respectively, $\mathrm{tr}(\bullet)$ yields the matrix trace, $\mathrm{etr}(\bullet)$ is a shorthand notation for $\exp(\mathrm{tr}(\bullet))$, while $\det(\bullet)$ and $|\bullet|$ will interchangeably denote the matrix determinant.

II. MIMO Channel Model and Joint Eigenvalue PDF

We consider a MIMO system with N_t transmit and N_r receive antennas and also define $s \triangleq \min(N_t, N_r)$ and $t \triangleq \max(N_t, N_r)$. In the case of flat Ricean fading, the channel matrix $\mathbf{H} \in \mathbb{C}^{N_r \times N_t}$ is modeled as [31]

$$\mathbf{H} = \sqrt{\frac{K}{K+1}}\mathbf{H}_{\mathrm{L}} + \sqrt{\frac{1}{K+1}}\mathbf{H}_w \tag{1}$$

where K is the Ricean K-factor expressing the ratio of powers of the free-space signal and the scattered waves. The random component, $\mathbf{H}_w$, accounts for the scattered signals with its entries being modeled as i.i.d. $\sim \mathcal{CN}(0,1)$ random variables (Rayleigh fading), while $\mathbf{H}_{\mathrm{L}}$ represents the deterministic non-fading component. We also define the physically measured SNR at each receiving antenna as γ while the channel power is normalized so that $\mathsf{E}\left[\mathrm{tr}\left(\mathbf{H}\mathbf{H}^\dagger\right)\right] = N_r N_t$. As was previously mentioned, we are particularly interested in optimized full-rank LoS configurations which can be realized by deploying specifically designed antenna arrays at both ends [9]–[13]. For the case of parallel uniform linear arrays (ULAs),[1] the optimum inter-element spacings at the Tx (d_t) and Rx (d_r) for a given Tx-Rx distance D and carrier wavelength λ, have to satisfy the following criterion [11, Eq. (28)]

$$d_t d_r \approx \lambda D\left(\frac{1}{t}+p\right),\ p \in \{0,1,2,...\}. \tag{2}$$

Although the above criterion is a function of terminal distance D, which may be unknown or constantly changing, it has been demonstrated in [11] that the sensitivity of the proposed configurations to displacements from the optimum is rather low. Hence, they can still achieve near-optimum performance over a large coverage area, which makes them likely to be employed in diverse modern applications, like suburban/indoor WLANs [32] or 60 GHz communications [33], to deliver ultra-broadband data rates. Another emerging applications are

[1]The case of tilted arrays admits a similar solution [11] but its study is beyond the scope of the paper.

typical point-to-point microwave links (i.e. between 6 and 38 GHz) and MIMO vehicular networks [34], where a moving vehicle communicates with either another vehicle or with the roadside in support of demanding applications spanning high-speed networking and video streaming to mobile commerce and Web surfing (see IEEE 802.11p standard).

A. Non-Central Wishart Matrices and Joint Eigenvalue PDF

From (1), we have that $E\{\mathbf{H}\} = \mathbf{M} = \sqrt{K/(K+1)}\mathbf{H}_{\mathrm{L}}$, while the column-correlation matrix of the random component is $\mathbf{\Sigma} = \varepsilon^2\mathbf{I}_s$, with $\varepsilon = 1/\sqrt{K+1}$. The instantaneous MIMO correlation matrix, $\mathbf{W}$, of the composite channel matrix is defined as

$$\mathbf{W} \triangleq \begin{cases} \mathbf{H}\mathbf{H}^{\dagger}, & \text{if } N_r \leq N_t \\ \mathbf{H}^{\dagger}\mathbf{H}, & \text{if } N_r > N_t. \end{cases} \tag{3}$$

In this case, $\mathbf{W} \in \mathbb{C}^{s\times s}$ follows an uncorrelated non-central Wishart distribution with t degrees of freedom, i.e. $\mathbf{W} \sim \mathcal{CW}_s\left(t, \varepsilon^2\mathbf{I}_s, \mathbf{\Omega}\right)$ [35], [36], where

$$\mathbf{\Omega} \triangleq \begin{cases} \mathbf{\Sigma}^{-1}\mathbf{M}\mathbf{M}^{\dagger}, & \text{if } N_r \leq N_t \\ \mathbf{\Sigma}^{-1}\mathbf{M}^{\dagger}\mathbf{M}, & \text{if } N_r > N_t \end{cases} \tag{4}$$

is the so-called non-centrality matrix. Hereafter, we consider a scaled version of $\mathbf{W}$, that is

$$\mathbf{S} = \mathbf{\Sigma}^{-1}\mathbf{W} \sim \mathcal{CW}_s\left(t, \mathbf{I}_s, \mathbf{\Omega}\right). \tag{5}$$

We denote its eigenvalues via $\boldsymbol{\lambda} \triangleq [\lambda_1, \lambda_2, \ldots, \lambda_s]^T$, with $\lambda_1 \geq \lambda_2 \ldots \geq \lambda_s > 0$. Likewise, we can define the eigenvalues of the non-centrality matrix, $\mathbf{\Omega}$, which are concatenated into the vector $\boldsymbol{\omega} \triangleq [\omega_1, \omega_2, \ldots, \omega_s]^T$. For the case of optimized LoS MIMO systems, the correlation between the LoS responses is eliminated, thereby resulting in orthogonal spatial LoS subchannels [9]–[13]. As such, the non-centrality matrix becomes diagonal and assuming that the relative differences in path loss are negligible, we end up with $\mathbf{\Omega} = t\mathbf{I}_s$, while its eigenvalues are $\omega_1 = \ldots = \omega_s = \omega = tK$. The joint ordered eigenvalue PDF of $\mathbf{S}$ in this limiting case is now given by the following theorem:

Theorem 1: The joint eigenvalue PDF of the uncorrelated non-central Wishart matrix $\mathbf{S}$ in (5) is

$$f(\boldsymbol{\lambda}) = c_1|\mathbf{\Psi}_c(\boldsymbol{\lambda})||\mathbf{\Phi}(\boldsymbol{\lambda})|\prod_{\ell=1}^{s}\lambda_\ell^{t-s}e^{-\lambda_\ell} \tag{6}$$

where $c_1 = \mathrm{etr}(-\boldsymbol{\omega})/\Gamma_s(s) = e^{-stK}/\Gamma_s(s)$, $\Gamma_m(n) = \prod_{i=1}^{m}(n-i)!$ and

$$\{\mathbf{\Phi}(\boldsymbol{\lambda})\}_{i,j} = \lambda_j^{s-i},\ \{\mathbf{\Psi}_c(\boldsymbol{\lambda})\}_{i,j} = \frac{\lambda_i^{s-j}}{(t-j)!}{}_0F_1(t+1-j;\lambda_i\omega) \tag{7}$$

while ${}_pF_q(\cdot)$ is the generalized hypergeometric function with p, q non-negative integers [37, Eq. (9.14.1)].

Proof: A detailed proof is given in Appendix A. ∎

III. MI MGF and Statistics

In this section, we explore the MIMO MI and provide exact and asymptotic high-SNR expressions for its first and second-order statistics. For the case of optimized LoS configurations with equal LoS eigenvalues, isotropic input has been shown to be capacity achieving even when the Tx knows the channel statistics [38, Proposition 1]. Based on this key observation and denoting the normalized SNR per transmitting antenna as $\gamma_c = \gamma\varepsilon^2/N_t$, the MI reads as [1]

$$I(\mathbf{H}) = \log_2\det\left(\mathbf{I}_{N_r} + \frac{\gamma}{N_t}\mathbf{H}\mathbf{H}^{\dagger}\right) = \sum_{\ell=1}^{s}\log_2\left(1+\gamma_c\lambda_\ell\right). \tag{8}$$

A. Exact MI Statistics

Assuming that the channel is ergodic, we can define the MI MGF according to (with $\mathbb{R}(\nu) < 0$)

$$G(\nu) = \mathsf{E}\left[\exp(\nu I(\mathbf{H}))\right] = \mathsf{E}\left[\prod_{\ell=1}^{s}(1+\gamma_c\lambda_\ell)^{\frac{\nu}{\ln 2}}\right] \tag{9}$$

while the expectation is across all channel realizations of $\mathbf{H}$.

Theorem 2: The MI MGF of the uncorrelated non-central Wishart matrix $\mathbf{S}$ in (5) is given by

$$G(\nu) = c_1\det\left(\mathbf{\Lambda}(\nu)\right) \tag{10}$$

where the entries of the $s\times s$ matrix $\mathbf{\Lambda}(\nu)$ are given by

$$\{\mathbf{\Lambda}(\nu)\}_{i,j} = \sum_{k=0}^{\infty}\frac{\alpha(k)!\omega^k\gamma_c^{-(\alpha(k)+1)}}{k!(t+k-j)!} \times U\left(\alpha(k)+1, \alpha(k)+2+\frac{\nu}{\ln 2}, \frac{1}{\gamma_c}\right) \tag{11}$$

with $\alpha(n) = t+s+n-i-j$, $\Gamma(x)$ is the well-known Gamma function and $U(a,b,z)$ is the Tricomi hypergeometric function [39, Eq. (13.1.3)].

Proof: The proof starts by invoking the integral definition of the MI MGF, that is

$$G(\nu) = \int_{D_0}\prod_{\ell=1}^{s}(1+\gamma_c\lambda_\ell)^{\frac{\nu}{\ln 2}}f(\boldsymbol{\lambda})d\lambda_1\ldots d\lambda_s \tag{12}$$

where $\mathcal{D}_0 = \{0 < \lambda_s < \ldots < \lambda_1 < \infty\}$. Substituting (6) into (12), and using the generic approach of [2, Corollary 2] to simplify the multiple integral into a scalar integral, we can reach the final result using [37, Eq. (9.211.4)] and after some basic algebraic manipulations. ∎

Theorem 3: The mean MI of the uncorrelated non-central Wishart matrix $\mathbf{S}$ in (5) reads

$$C = \mathsf{E}\left[I(\mathbf{H})\right] = \frac{c_1e^{1/\gamma_c}}{\ln 2}\sum_{\ell=1}^{s}\det\left(\mathbf{\Lambda}_c(\ell)\right) \tag{13}$$

where the entries of the $s\times s$ matrix $\mathbf{\Lambda}_{\mathrm{c}}(\ell)$ are

$$\{\mathbf{\Lambda}_{\mathrm{c}}(\ell)\}_{i,j} = \begin{cases} \displaystyle\sum_{k=0}^{\infty}\frac{\alpha(k)!\omega^k\Delta_1(\alpha(k)+1,\rho_c)}{k!(t+k-j)!}, & j = \ell \\ (t+s-i-j)!/(t-j)! & \\ \times{}_1F_1(t+s-i-j+1; t-j+1; \omega), & j \neq \ell \end{cases} \tag{14}$$

where

$$\Delta_1(m,\beta) = \sum_{i=1}^{m}\frac{\Gamma(-m+i, 1/\beta)}{\beta^{m-i}} = \sum_{i=0}^{m-1}\mathbb{E}_{i+1}(1/\beta) \tag{15}$$

with $\Gamma(p,x) = \int_x^\infty t^{p-1}e^{-t}dt$ being the upper incomplete gamma function [37, Eq. (8.350.2)] while $\mathbb{E}_n(z) = \int_1^\infty t^{-n}e^{-zt}dt,\ n = 0,1,2,\ldots,\mathbb{R}(z) > 0$ is the exponential integral function [39, Eq. (5.1.4)].

Proof: The proof is based on the definition of the n-th order moment of MI, or

$$\mathsf{E}\left[I(\mathbf{H})^n\right] = \left.\frac{d^n(G(\nu))}{d\nu^n}\right|_{\nu=0}. \tag{16}$$

Setting $n = 1$ in (16), and using the product rule for the derivative of a determinant in (11), we can obtain the desired result after introducing the Lebesque's Dominated Convergence Theorem [40, Sec. 5.9] to interchange the order of integration and differentiation, and with the aid of [6, Eq. (40)]. ∎

For the convergence of the infinite series in (14), we will now assume that $T_0 - 1$ terms are used so that the truncation error $\mathcal{R}_0$ can be written as

$$\begin{aligned}\mathcal{R}_0 &= \sum_{k=T_0}^{\infty} \frac{\alpha(k)!\omega^k \Delta_1(\alpha(k)+1,\gamma_c)}{k!(t+k-j)!} \\ &< \sum_{k=T_0}^{\infty} \frac{\alpha(k)!\omega^k(\alpha(k)+1)\mathbb{E}_1(1/\gamma_c)}{k!(t+k-j)!} \\ &< \frac{\mathbb{E}_1(1/\gamma_c)\omega^{T_0}(t+s+T_0-i-j+1)!}{T_0!(t+T_0-j)!} \\ &\times {}_2F_2(t+s+T_0-i-j+2,1;T_0+1,t+T_0-j+1;\omega)\end{aligned}$$

where we have used the fact that $\mathbb{E}_n(1/\beta)$ is a monotonically decreasing function in n.

The following theorem returns the second MI moment, through which we can obtain the MI variance:

$$\mathsf{Var}(I(\mathbf{H})) = \mathsf{E}\left[I(\mathbf{H})^2\right] - \left(\mathsf{E}\left[I(\mathbf{H})\right]\right)^2. \tag{17}$$

Theorem 4: The second MI moment of the uncorrelated non-central Wishart matrix $\mathbf{S}$ in (5) reads

$$E\left[I(\mathbf{H})^2\right] = \frac{c_1}{(\ln 2)^2}\sum_{\ell=1}^{s}\sum_{n=1}^{s}\det\left(\mathbf{\Lambda}_{\mathrm{v}}(\ell,n)\right) \tag{18}$$

where the entries of the $s \times s$ matrix $\mathbf{\Lambda}_{\mathrm{v}}(\ell,n)$ are given in (19) at the top of next page, with [6, Eq. (41)]

$$\begin{aligned}\Delta_2(m,b) &= \int_0^\infty y^{m-1}\ln^2(1+by)e^{-y}dy = \frac{2e^{\frac{1}{b}}}{b^m} \\ &\times \sum_{p=0}^{m-1}(-1)^p\binom{m-1}{p}G_{3,4}^{4,0}\left[\frac{1}{b}\,\middle|\,\begin{matrix}p-(m-1),p-(m-1),p-(m-1)\\ 0,p-m,p-m,p-m\end{matrix}\right]\end{aligned} \tag{20}$$

where $G_{p,q}^{m,n}\left[x,\left|\begin{matrix}\alpha_1,\ldots,\alpha_p\\ \beta_1,\ldots,\beta_q\end{matrix}\right.\right]$ is the Meijer's G-function [37, Eq. (9.301)].

Proof: The proof follows a similar line of reasoning as in Theorem 3, by simply setting $n = 2$ in (16) and using the well-known properties for the second-order derivatives of determinants. ∎

For the convergence of (19)–(20), we first note that the integrand in (20) is dominated by the exponential term as $y \to \infty$. Hence, we can split the integral into two integrals over $[0, A]$ and (A, ∞) with $A > 0$ such that the latter term becomes infinitely small. The first integral can be further split and upper bounded using the monotonicity wrt y and $\alpha(k)$ of the individual terms in the integrand of (20). After some algebra, it can be shown that $\exists c > 0, \Delta_2(\alpha(k)+1,\gamma_c) < cA^{\alpha(k)}$ which concludes the proof for the series convergence. Note that the integral in (20) admits an alternative closed-form solution via a mixture of hypergeometric/exponential integral functions as given in [41, Eq. (20)].

B. Asymptotic High-SNR MI Statistics

We can now investigate the MI statistics in the high-SNR regime. A straightforward option is to take γ infinitely large in (13)–(15) and (18)–(20), as was done in a conference version of this paper [13]. We herein, however, adopt an alternative approach in order to obtain more insightful results regarding the parameters that affect the MI statistics. Note that our analysis uses similar arguments to [16]. On this basis, the key point of our analysis is the following lemma which returns the υ-th moment of the generalized variance of $\mathbf{W}$:

Lemma 1: The υ-th moment of the generalized variance of $\mathbf{W} \sim \mathcal{CW}_s\left(t, \varepsilon^2\mathbf{I}_s, \mathbf{\Omega}\right)$ is given by

$$\phi(\upsilon) = \mathsf{E}\left[|\mathbf{W}|^\upsilon\right] = \varepsilon^{2s\upsilon}\frac{c_1\Gamma_s(t+\upsilon)}{\Gamma_s(t)}|\mathbf{A}(\upsilon)| \tag{21}$$

where $\mathbf{A}(\upsilon)$ is a $s \times s$ real matrix with entries

$$\{\mathbf{A}(\upsilon)\}_{i,j} = \begin{cases} {}_2F_2(t+\upsilon-s+i,i;t-s+i,i-j+1;\omega) \\ \times\frac{\omega^{i-j}(i-1)!}{(i-j)!}, & i \geq j \\ {}_2F_2(t+\upsilon-s+j,j;t-s+j,j-i+1;\omega) \\ \times\frac{(t-s+i-1)!(t+\upsilon-s+j-1)!(j-1)!}{(t-s+j-1)!(t+\upsilon-s+i-1)!(j-i)!} & i < j. \end{cases} \tag{22}$$

Proof: A detailed proof is given in Appendix B-A. ∎

Theorem 5: As $\gamma \to \infty$, the mean MI in (8) tends to

$$\begin{aligned}\mathsf{E}\left[I^\infty(\mathbf{H})\right] &= s\log_2\left(\frac{\gamma}{N_t}\right) + \frac{1}{\ln 2}\sum_{k=0}^{s-1}\psi(t-k) \\ &+ s\log_2(\varepsilon^2) + \frac{1}{\ln 2}\frac{\sum_{\ell=1}^{s}|\mathbf{B}(\ell)|}{|\mathbf{A}(0)|}\end{aligned} \tag{23}$$

where $\psi(x)$ is the digamma function [37, Eq. (8.360.1)] and $\mathbf{B}(\ell) \in \mathbb{R}^{s\times s}$ is defined as

$$\{\mathbf{B}(\ell)\}_{i,j} = \begin{cases} \{\mathbf{A}(0)\}_{i,j}, & j \neq \ell \\ \sum_{k=1}^{\infty}\frac{(k+i-1)!}{(k+i-j)!}\frac{\omega^{k+i-j}}{k!}\left(\sum_{n=0}^{k-1}\frac{1}{t-s+i+n}\right), & \\ & j = \ell,\ i \geq j \\ \sum_{k=0}^{\infty}\frac{(k+j-1)!}{(k+j-i)!}\frac{\omega^k}{k!}\left(\sum_{n=0}^{k+j-i-1}\frac{1}{t-s+i+n}\right), & \\ & j = \ell,\ i < j. \end{cases} \tag{24}$$

Proof: A detailed proof is given in Appendix B-B. ∎

The above theorem validates a classical result for MIMO systems, which states that at high SNRs the mean MI increases linearly with the minimum number of transmit/receive antennas [1], [3]–[5]. In addition, we can see that at high SNRs the effects of Rayleigh/Ricean fading are decoupled.

$$\{\mathbf{\Lambda}_{\mathrm{v}}(\ell,n)\}_{i,j}=\begin{cases}\displaystyle\sum_{k=0}^{\infty}\frac{\omega^k\Delta_2(\alpha(k)+1,\gamma_c)}{k!(t+k-j)!}, & j=\ell=n\\ \displaystyle\sum_{k=0}^{\infty}\frac{\alpha(k)!\omega^k\Delta_1(\alpha(k)+1,\gamma_c)}{k!(t+k-j)!}, & j=\ell \text{ or } j=n,\ \ell\neq n\\ (t+s-i-j)!{}_1F_1(t+s-i-j+1;t-j+1;\omega)/(t-j)!, & j\neq\ell, j\neq n\end{cases} \tag{19}$$

Theorem 6: As $\gamma\to\infty$, the MI variance in (8) tends to

$$\mathsf{Var}\left[I^{\infty}(\mathbf{H})\right]=\frac{1}{(\ln 2)^2}\left(\sum_{k=0}^{s-1}\psi'(t-k)-\left(\frac{\sum_{\ell=1}^{s}|\mathbf{B}(\ell)|}{|\mathbf{A}(0)|}\right)^2+\frac{\sum_{\ell=1}^{s}\sum_{p=1,p\neq\ell}^{s}|\mathbf{C}(\ell,p)|}{|\mathbf{A}(0)|}+\frac{\sum_{\ell=1}^{s}|\mathbf{D}(\ell)|}{|\mathbf{A}(0)|}\right) \tag{25}$$

where $\mathbf{C}(\ell,p),\mathbf{D}(\ell)$ are real $s\times s$ matrices with entries defined in (26)–(27) at the top of next page

Proof: A detailed proof is given in Appendix B-C. ■

Clearly, the asymptotic MI variance is independent of the SNR. This demonstrates explicitly that the variance of the MIMO MI converges to a deterministic constant as the SNR grows infinitely large, which is consistent with the results of [3], [16]. For Rayleigh fading ($K=0,\mathbf{\Omega}=\mathbf{0}$), the asymptotic MI statistics (23) and (25) simplify to

$$\mathsf{E}\left[I^{\infty}(\mathbf{H})\right] = s\log_2\left(\frac{\gamma}{N_t}\right)+\frac{1}{\ln 2}\sum_{k=0}^{s-1}\psi(t-k) \tag{28}$$

$$\mathsf{Var}\left[I^{\infty}(\mathbf{H})\right] = \frac{1}{(\ln 2)^2}\sum_{k=0}^{s-1}\psi'(t-k) \tag{29}$$

which are respectively in agreement with [3, Eq. (9)], [5, Eq. (12)] and [5, Eq. (31)], [16, Eq. (105)].

C. Outage Capacity-Gaussian Approximation

The Gaussian approximation for the MI distribution was originally proposed in [42] for the case of i.i.d. Rayleigh channels and thereafter adopted for various types of correlated Rayleigh/Ricean MIMO channels [6], [16], [21]. The key implication of this approximation, is that the outage capacity, $I_{\text{out}}(\alpha)$, can be directly obtained via the MI mean and variance as derived in Theorems 3 and 4. Hence, we can write

$$I_{\text{out}}(\alpha)=\mathsf{E}\left[I(\mathbf{H})\right]+\sqrt{\mathsf{Var}\left[I(\mathbf{H})\right]}Q^{-1}(\alpha) \tag{30}$$

with $Q^{-1}(\cdot)$ being the inverse Gaussian Q-function while α represents the outage probability, or the largest information rate of reliable communications that is guaranteed at $100(1-\alpha)\%$ of the cases. In our numerical results, we demonstrate that the Gaussian approximation works quite well for optimized LoS MIMO configurations under different channel parameters.

IV. Performance Analysis of Optimum Linear Transceivers for MBF MIMO Systems

We now elaborate on the performance of the optimum eigenfilters in a typical MBF MIMO system with perfect CSI at both ends. For this reason, we will use the common system model of [22] (adopted also in [23]–[25]), without giving explicit details due to space constraints. The main idea is that when a precoder matrix $\mathbf{B}\in\mathbb{C}^{N_t\times r}$ is applied to the transmit side, with $r\leq s$ denoting the number of modulated data symbols, the optimum transmit-receive spatial filter (after equalization) is identified by the Wiener solution:

$$\mathbf{A}\triangleq(\mathbf{HBB}^{\dagger}\mathbf{H}^{\dagger}+\mathbf{I}_{N_r})^{-1}\mathbf{HB}. \tag{31}$$

More importantly, the optimum transmit matrix $\mathbf{B}$ is inherently related to the channel eigenmodes via

$$\mathbf{B}\triangleq\mathbf{UP} \tag{32}$$

where $\mathbf{U}\in\mathbb{C}^{N_t\times r}$ is a matrix whose columns are the r dominant eigenvectors of $\mathbf{H}^{\dagger}\mathbf{H}$ while $\mathbf{P}=\mathrm{diag}\{\sqrt{p_i}\}_{i=1}^{r}$ is a diagonal power allocation matrix whose entries fulfill the constraint $\sum_{i=1}^{r}p_i=\gamma$. Then, it has been shown [22], [23], [25] that the instantaneous SNR across the k-th eigenmode is

$$\gamma_k=\varepsilon^2\lambda_k p_k,\quad k=1,\ldots,r. \tag{33}$$

The above equation implies that the eigenmode SNR is a function of the corresponding marginal eigenvalue of the instantaneous correlation matrix. Thus, it is critical to examine the marginal/unordered eigenvalue distributions for which we now derive exact and asymptotic closed-form expressions. As before, our starting point is the joint eigenvalue PDF in (6) although the following analytic expressions can be also obtained by particularizing the results of [26]–[28] to the specific case of equal LoS eigenvalues.

Theorem 7: The CDF/PDF of the maximum eigenvalue λ_1 of the uncorrelated non-central Wishart matrix $\mathbf{S}$ in (5) are respectively given by

$$F_{\lambda_1}(x) = \Pr(\lambda_1\leq x)=c_1|\mathbf{\Xi}(x)| \tag{34}$$

$$f_{\lambda_1}(\lambda_1) = c_1\sum_{\ell=1}^{s}|\mathbf{\Xi}_{\ell}(\lambda_1)| \tag{35}$$

where $\mathbf{\Xi}(x)$ and $\mathbf{\Xi}_{\ell}(\lambda_1)$ are $s\times s$ matrices with entries

$$\{\mathbf{\Xi}(x)\}_{i,j}=\sum_{k=0}^{\infty}\frac{\omega^k\gamma(t+k+s-i-j+1,x)}{k!(t+k-j)!} \tag{36}$$

$$\{\mathbf{\Xi}_{\ell}(\lambda_1)\}_{i,j}=\begin{cases}\dfrac{e^{-\lambda_1}\lambda_1^{t+s-i-j}}{(t-j)!}{}_0F_1(t-j+1;\omega\lambda_1), & j=\ell\\ \{\mathbf{\Xi}(\lambda_1)\}_{i,j}, & j\neq\ell\end{cases} \tag{37}$$

with $\gamma(p,x)=\int_0^x t^{p-1}e^{-t}dt$ being the lower incomplete gamma function [37, Eq. (8.350.1)].

Proof: In order to evaluate this probability, we employ

$$\{\mathbf{C}(\ell,p)\}_{i,j} = \begin{cases} \{\mathbf{A}(0)\}_{i,j}, & j\neq\ell,\ j\neq p \\ \sum_{k=1}^{\infty}\frac{(k+i-1)!}{(k+i-j)!}\frac{\omega^{k+i-j}}{k!}\left(\sum_{n=0}^{k-1}\frac{1}{t-s+i+n}\right), & j=\ell \text{ or } j=p,\ i\geq j \\ \sum_{k=0}^{\infty}\frac{(k+j-1)!}{(k+j-i)!}\frac{\omega^{k}}{k!}\left(\sum_{n=0}^{k+j-i-1}\frac{1}{t-s+i+n}\right), & j=\ell \text{ or } j=p,\ i<j \end{cases} \quad (26)$$

$$\{\mathbf{D}(\ell)\}_{i,j} = \begin{cases} \{\mathbf{A}(0)\}_{i,j}, & j\neq\ell \\ \sum_{k=2}^{\infty}\frac{(k+i-1)!}{(k+i-j)!}\frac{\omega^{k+i-j}}{k!}\left(\sum_{n=0}^{k-2}\sum_{m=n+1}^{k-1}\frac{2}{(t-s+i+n)(t-s+i+m)}\right), & j=\ell,\ i\geq j \\ \sum_{k=0}^{\infty}\frac{(k+j-1)!}{(k+j-i)!}\frac{\omega^{k}}{k!}\left(\sum_{n=\max(0,i-j+2)}^{k+j-i-2}\sum_{m=n+1}^{k+j-i-1}\frac{2}{(t-s+i+n)(t-s+i+m)}\right), & j=\ell,\ i<j \end{cases} \quad (27)$$

its integral definition, that is

$$F_{\lambda_1}(x) = \Pr(\lambda_s < \ldots \lambda_1 \leq x) = \int_{D_1} f(\boldsymbol{\lambda}) d\lambda_1 \ldots d\lambda_s \quad (38)$$

with $\mathcal{D}_1 = \{\lambda_s < \ldots < \lambda_1 < x\}$. From inspection, the above integral is of the same type as the one in (12). This implies that the same technique can be applied for tackling the product of determinants in (6). The result follows trivially by using the multilinear property of a determinant as in (12) and invoking the definition of $\gamma(p,x)$. The PDF expression is obtained by differentiating (34) with respect to (wrt) x. ∎

The truncation error, $\mathcal{R}_1$, for the infinite series in (36) if $T_1 - 1$ terms are used, is expressed as

$$\begin{aligned}\mathcal{R}_1 &= \sum_{k=T_1}^{\infty}\frac{\omega^k\gamma(t+k+s-i-j+1,x)}{k!(t+k-j)!} \\ &= \sum_{k=T_1}^{\infty}\frac{\omega^k x^{(\alpha(k)+1)}{}_1F_1(\alpha(k)+1;\alpha(k)+2;-x)}{k!(t+k-j)!(\alpha(k)+1)} \\ &< \frac{\omega^{T_1}x^{(\alpha(T_1)+1)}{}_1F_1\left(\alpha(T_1)+1;\alpha(T_1)+2;-x\right)}{T_1!(t+T_1-j)!(\alpha(T_1)+1)} \\ &\quad\times {}_2F_3(\alpha(T_1)+1,1;T_1+1,t+T_1-j+1,\alpha(T_1)+2;\omega x)\end{aligned}$$

where the second line follows from $\gamma(\alpha,y) = y^{\alpha}{}_1F_1(\alpha;\alpha+1;-y)/\alpha$ [39, Eq. (6.5.12)] and the third since ${}_1F_1(\alpha;\alpha+1;-y)$ is a monotonically decreasing function in α for all positive values of α and y. Note that (34) can be alternatively obtained via [43, Eq. (2)] with the aid of [30, Lemma 2].

Theorem 8: The CDF/PDF of the minimum eigenvalue λ_s of the uncorrelated non-central Wishart matrix $\mathbf{S}$ in (5) are respectively given by

$$F_{\lambda_s}(x) = \Pr(\lambda_s \leq x) = 1 - c_1|\boldsymbol{\Theta}(x)| \quad (39)$$

$$f_{\lambda_s}(\lambda_s) = c_1\sum_{\ell=1}^{s}|\boldsymbol{\Theta}_\ell(\lambda_s)| \quad (40)$$

where $\boldsymbol{\Theta}(x)$ and $\boldsymbol{\Theta}_\ell(\lambda_s)$ are $s\times s$ matrices with entries

$$\{\boldsymbol{\Theta}(x)\}_{i,j} = \sum_{k=0}^{\infty}\frac{\omega^k\Gamma(t+k+s-i-j+1,x)}{k!(t+k-j)!} \quad (41)$$

$$\{\boldsymbol{\Theta}_\ell(\lambda_s)\}_{i,j} = \begin{cases}\{\boldsymbol{\Xi}_\ell(\lambda_s)\}_{i,j}, & j=\ell \\ \{\boldsymbol{\Theta}(\lambda_s)\}_{i,j}, & j\neq\ell.\end{cases} \quad (42)$$

Proof: The proof follows a similar line of reasoning as in Theorem 7 with the only difference pertaining to the integration region since we now have that

$$\begin{aligned}F_{\lambda_s}(x) &= 1 - \Pr(\lambda_1 > \ldots \lambda_s > x) \\ &= 1 - \int_{D_2} f(\boldsymbol{\lambda}) d\lambda_1 \ldots d\lambda_s \end{aligned} \quad (43)$$

with $\mathcal{D}_2 = \{x < \lambda_s < \ldots < \lambda_1\}$. The PDF expression is obtained by differentiating (39) wrt x. ∎

We note that since $\{\boldsymbol{\Theta}(x)\}_{i,j} = {}_1F_1(t+s-i-j+1;t-j+1;\omega)(t+s-i-j)!/(t-j)! - \{\boldsymbol{\Xi}(x)\}_{i,j}$, we can express the absolute truncation error, $\mathcal{R}_2$, of (41) simply as $\mathcal{R}_2 = |\mathcal{R}_1|$.

Theorem 9: The CDF of the k-th ($k\geq 2$) largest eigenvalue λ_k of the uncorrelated non-central Wishart matrix $\mathbf{S}$ in (5) is

$$F_{\lambda_k}(x) = \Pr(\lambda_k \leq x) = F_{\lambda_{k-1}}(x) + c_1\sum_{1}|\boldsymbol{\Omega}(x)| \quad (44)$$

where $\sum_1$ represents the sum over all $(\alpha_1,\ldots,\alpha_s)$ satisfying $(\alpha_1 < \ldots < \alpha_{k-1})$ and $(\alpha_k < \ldots < \alpha_s)$ with $(\alpha_1,\ldots,\alpha_s)$ being a permutation of $(1,\ldots,s)$, while $\boldsymbol{\Omega}(x)$ is an $s\times s$ matrix with entries

$$\{\boldsymbol{\Omega}(x)\}_{\alpha_i,j} = \begin{cases}\{\boldsymbol{\Theta}(x)\}_{\alpha_i,j}, & i=1,\ldots,k-1 \\ \{\boldsymbol{\Xi}(x)\}_{\alpha_i,j}, & i=k,\ldots,s.\end{cases} \quad (45)$$

Proof: The proof stems directly from Theorems 7 and 8 using the approach of [25, Theorem 3]. ∎

The PDF expression for the k-th eigenvalue follows by differentiating (44) wrt x where for the derivative of $|\boldsymbol{\Omega}(x)|$ we can use (37) and (42) and the properties for the first derivative of a determinant. Due to the notation being cumbersome however, we do not present the final expression in this paper.

Apart from the ordered eigenvalues, an equally important feature of MIMO systems is the unordered (generic) eigenvalue of $\mathbf{S}$, whose PDF can lead to the ergodic capacity as originally demonstrated in [1].

Theorem 10: The PDF of the unordered eigenvalue λ of the uncorrelated non-central Wishart matrix $\mathbf{S}$ in (5) is

$$\begin{aligned}f_\lambda(\lambda) = \frac{c_1}{s}\sum_{n=1}^{s}\sum_{m=1}^{s}(-1)^{m+n}&\frac{\lambda^{t+s-m-n}{}_0F_1(t-m+1;\lambda\omega)}{(t-m)!} \\ &\times e^{-\lambda}\left|\boldsymbol{\Pi}(m,n,\omega)\right|\end{aligned}$$

where $\boldsymbol{\Pi}(m,n,\omega)\in\mathbb{R}^{(s-1)\times(s-1)}$ is defined as

$$\begin{aligned}\{\boldsymbol{\Pi}(n,m,\omega)\}_{i,j} = &\frac{(t+s-r_{j,m}-r_{i,n})!}{(t-r_{j,m})!} \\ &\times {}_1F_1(t+s-r_{j,m}-r_{i,n}+1,t-r_{j,m}+1;\omega)\end{aligned} \quad (46)$$

with

$$r_{x,y} \triangleq \begin{cases}x, & \text{if } x<y \\ x+1, & \text{if } x\geq y.\end{cases} \quad (47)$$

Proof: The proof is based on applying the framework of [26] to the joint ordered eigenvalue PDF (6). To this end, we first express the generic eigenvalue λ as

$$f_\lambda(\lambda) = \int_0^\infty \int_0^\infty \cdots \int_0^\infty \frac{f(\boldsymbol{\lambda})}{s!} \mathrm{d}\lambda_s \ldots \mathrm{d}\lambda_3 \mathrm{d}\lambda_2 \qquad (48)$$

where we have used the property that the unordered joint eigenvalue PDF is $f(\boldsymbol{\lambda})/s!$. Substituting the involved determinants from (7) into (48) and thereafter introducing [26, Corollary 1, Eq. (21)], we can obtain the desired result after solving the resulting integral using [37, Eq. (7.52.5)]

$$\int_0^\infty e^{-x} x^{\nu-1} {}_pF_q\left(a_1, \ldots, a_p; b_1, \ldots, b_q; \alpha x\right) = \Gamma(\nu) {}_{p+1}F_q\left(\nu, a_1, \ldots, a_p; b_1, \ldots, b_q; \alpha\right)$$

for $p < q$ and $\mathbb{R}(\nu) > 0$. ∎

It is interesting to note that the expression (13) for the exact mean MI can be alternatively obtained by combining Telatar's approach [1] with Theorem 10 via the relationship:

$$\mathsf{E}\left[I(\mathbf{H})\right] = \frac{s}{\ln 2} \int_0^\infty \log(1+\gamma_c u) f_\lambda(u) \mathrm{d}u. \qquad (49)$$

A. Asymptotic Marginal Eigenvalue Expressions

We hereafter derive first-order expansions for the marginal eigenvalue distributions of the ordered eigenvalues $\lambda_k, k = 1, \ldots, s$. These expressions will be particularly useful when analyzing the asymptotic performance of MIMO systems for small outage (e.g. 0.01, 0.001). We begin with the following theorem:

Theorem 11: The first-order expansions of the CDF/PDF of the k-th ($k \geq 2$) largest eigenvalue λ_k of the uncorrelated non-central Wishart matrix $\mathbf{S}$ in (5) around $\lambda_k = 0^+$ are

$$F_{\lambda_k}(\lambda_k) = c_1 \lambda_k^{(t-k+1)(s-k+1)} \frac{|\boldsymbol{\Delta}_1||\boldsymbol{\Delta}_2|}{\Gamma_s(t)} + o\left(\lambda_k^{(t-k+1)(s-k+1)}\right) \qquad (50)$$

$$f_{\lambda_k}(\lambda_k) = c_1 (t-k+1)(s-k+1) \lambda_k^{(t-k+1)(s-k+1)-1} \times \frac{|\boldsymbol{\Delta}_1||\boldsymbol{\Delta}_2|}{\Gamma_s(t)} + o\left(\lambda_k^{(t-k+1)(s-k+1)-1}\right) \qquad (51)$$

where the involved matrices $\boldsymbol{\Delta}_1 \in \mathbb{R}^{(k-1)\times(k-1)}$ and $\boldsymbol{\Delta}_2 \in \mathbb{R}^{(s-k+1)\times(s-k+1)}$ are respectively defined as

$$\{\boldsymbol{\Delta}_1\}_{i,j} = (t+s-i-j)! \times {}_1F_1(t+s-i-j+1; t-j+1; \omega) \qquad (52)$$

$$\{\boldsymbol{\Delta}_2\}_{i,j} = \frac{1}{t+s-2k+3-i-j}. \qquad (53)$$

Proof: A detailed proof is given in Appendix C. ∎

Corollary 1: The first-order expansions of the CDF/PDF of the maximum eigenvalue λ_1 of the uncorrelated non-central Wishart matrix $\mathbf{S}$ in (5) around $\lambda_1 = 0^+$ are respectively given by

$$F_{\lambda_1}(\lambda_1) = \frac{\Gamma_s(s)}{\Gamma_s(t+s)} e^{-stK} \lambda_1^{st} + o(\lambda_1^{st}) \qquad (54)$$

$$f_{\lambda_1}(\lambda_1) = \frac{st\Gamma_s(s)}{\Gamma_s(t+s)} e^{-stK} \lambda_1^{st-1} + o(\lambda_1^{st-1}). \qquad (55)$$

Proof: The proof uses similar methodology as above, with the starting point being (34) for the exact CDF of λ_1. The same result can be obtained by setting $k = 1$ in (50) and noting that $|\boldsymbol{\Delta}_2| = |1/(t+s-i-j+1)| = \Gamma_s(s)^2 \Gamma_s(t)/\Gamma_s(t+s)$. The expression in (55) is obtained by differentiating (54) wrt λ_1. ∎

We point out the similarity of (54)–(55) with the corresponding expressions for the case of distinct LoS eigenvalues with rank-L ($L \leq s$) mean channel matrix [16, Theorem 4]. This implies that the rank of the mean channel matrix has no impact on the asymptotic performance of λ_1. This observation is critical when assessing the performance of maximum ratio combiners (MRC) where all power is allocated to the dominant eigenmode. From (50), we can infer that for a given total number of antennas $t+s$, the optimum choice in terms of outage is to maximize ts, or equivalently to evenly distribute the number of antennas at both ends, i.e. $N_t = N_r$. The same conclusion stems from (54) and is in agreement with [43].

B. Statistics of the Eigenmode SNR: Outage Probability and PDF

In general, the outage probability is a critical metric in the performance evaluation of all communication systems, since it indicates the probability that the SNR falls below a predefined threshold, γ_{th}. Its study has been thoroughly addressed in different papers for various fading scenarios (e.g. [44], [45]). For the considered problem, we will assume that power is uniformly distributed across all active subchannels so that $p_k = \gamma/r$. Then, recalling (33), we can express the outage of the k-th eigenmode, $P_{\text{out},k}$, as

$$P_{\text{out},k} \triangleq \Pr(\gamma_k \leq \gamma_{\text{th}}) = \Pr\left(\lambda_k \leq \frac{\gamma_{\text{th}}}{\varepsilon^2 p_k}\right) = F_{\lambda_k}\left(\frac{\gamma_{\text{th}}(K+1)r}{\gamma}\right), \quad k = 1, \ldots, r. \qquad (56)$$

Combining (56) with (34), (39) and (44) we can get analytical expressions for the outage of any MIMO eigenmode. For small outage probabilities the asymptotic expressions in (50) and (54) can be invoked:

$$P_{\text{out},k}^{\infty} = \frac{c_1 |\boldsymbol{\Delta}_1||\boldsymbol{\Delta}_2|}{\Gamma_s(t)} \left(\frac{\gamma_{\text{th}}(K+1)r}{\gamma}\right)^{(t-k+1)(s-k+1)} + o\left(\left(\frac{\gamma_{\text{th}}(K+1)r}{\gamma}\right)^{(t-k+1)(s-k+1)}\right), \; k \geq 2 \qquad (57)$$

$$P_{\text{out},k}^{\infty} = \frac{\Gamma_s(s)}{\Gamma_s(t+s)} e^{-stK} \left(\frac{\gamma_{\text{th}}(K+1)r}{\gamma}\right)^{st} + o\left(\frac{\gamma_{\text{th}}(K+1)r}{\gamma}\right)^{st}, \; k = 1. \qquad (58)$$

In addition, the eigenmode SNR PDF can be readily obtained as follows

$$f_{\gamma_k}(\gamma_k) = \left(\frac{(K+1)r}{\gamma}\right) f_{\lambda_k}\left(\frac{\gamma_k(K+1)r}{\gamma}\right), \quad k = 1, \ldots, r. \qquad (59)$$

V. Numerical Results

In this section, the theoretical results presented in Sections III and IV are validated. To this end, 10^5 random real-

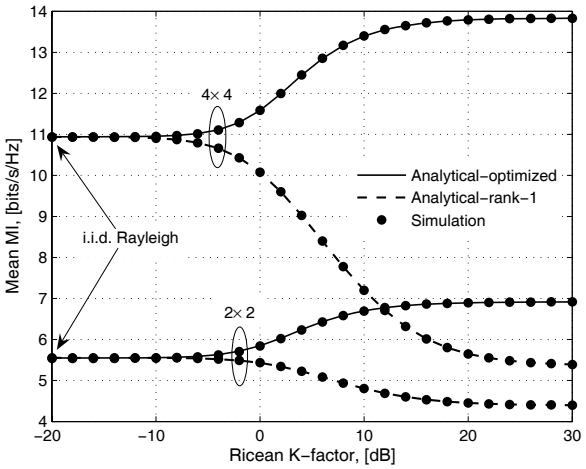

Fig. 1. Analytical and simulated mean MI of optimized and conventional MIMO configurations against the Ricean K-factor ($\gamma = 10$ dB).

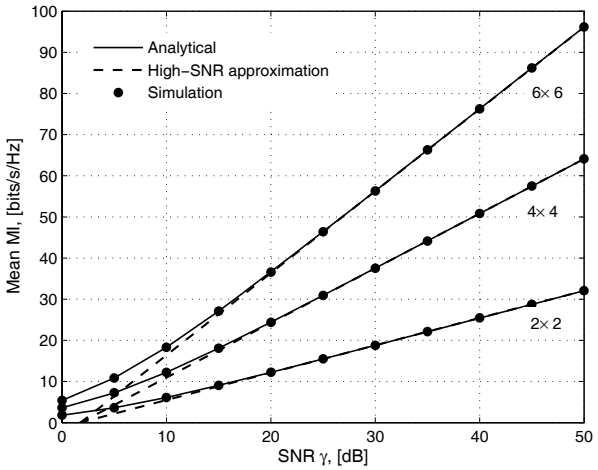

Fig. 2. Analytical, high-SNR approximation and simulated mean MI against the SNR, γ ($K = 3$ dB).

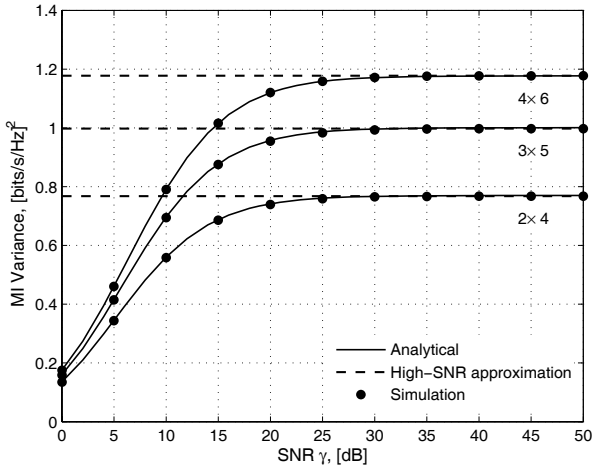

Fig. 3. Analytical, high-SNR approximation and simulated MI variance against the SNR, γ ($K = 3$ dB).

izations of the channel matrix $\mathbf{H}$ are generated according to (1), assuming $d_t = d_r$, for each K-factor under consideration (carrier frequency 5.2 GHz, $D = 5$ m). We first investigate the effects of deterministic components on the mean MI. In order to get a better understanding, our analysis also considers a conventional rank-1 mean channel matrix with spacings $d_t = d_r = \lambda/2$.

In Fig. 1, the ergodic capacity is depicted against the K-factor assuming both optimized/conventional structures for the mean channel matrix. The theoretical curves are based on Theorem 3 for the former case and [6, Eq. (37)] for the latter.

It is observed that the match between theory and simulation is excellent in all cases under consideration, thereby validating the correctness of the proposed analytical expressions. The graph clearly contradicts the common belief that the presence of LoS components reduces the advantages of MIMO technology due to limited amount of scattering, compared to Rayleigh fading conditions. As K gets higher, optimized configurations offer the maximum MIMO capacity. In fact, with no transmit CSI and under UPA any configuration of arbitrary rank will deliver a capacity between these two extremes. On the other hand, for $K \leq 0$ dB the advantages of optimized configurations diminish and in the limit, $K \to -\infty$ dB, the LoS component vanishes and we end up with a pure i.i.d. Rayleigh channel. These results are consistent with [9]–[13].

In Fig. 2, the mean MI is illustrated against the SNR, γ, for a given $K = 3$ dB and three different MIMO setups. The outputs of a Monte-Carlo simulator are compared with the exact and asymptotic high-SNR expressions of Theorem 3 and 5, respectively. Once more, there is an exact agreement between the analytical curves and the Monte-Carlo simulations; further, the high-SNR expressions become sufficiently tight at $\gamma \geq 15$ dB and thus can explicitly predict the mean MI for most practical SNR values.

Fig. 3 investigates the effects of SNR/number of antennas on the MI variance. The exact and high-SNR expressions of Theorem 4 and 6, are respectively considered. Both parameters tend to increase the channel randomness, though for high SNR the variance is much smaller than the mean [21]. As expected, the asymptotic curve is independent of the SNR and also becomes exact at moderate SNRs, especially when small MIMO systems are deployed. These observations are in line with [6], [16], [21].

In Fig. 4, the accuracy of the Gaussian approximation introduced in Section III-C is tested. The analytical curves are overlaid with the simulation results. The match is precise for all cases, even when the number of antennas is low, which highlights the importance of the analytical expressions for the MI mean and variance in the context of outage capacity characterization. A higher K-factor shifts the PDFs to the right (higher mean) and in parallel reduces the MI variance (i.e. more deterministic channels).

In the second part of the evaluation process, we consider the MBF performance of optimized LoS MIMO configurations. We first verify the analytical marginal eigenvalue expressions as given in Theorems 7–9 for a 3×8 MIMO system (c.f. Fig. 5). In all cases, the match is exact while all eigenvalues benefit from a higher K-factor (i.e. enhanced channel conditioning and thus link stabilization) which is in fundamental contrast with rank-deficient configurations where only a subset of eigenmodes is fostered by strong LoS components.

Fig. 6 more closely addresses the individual eigenmode

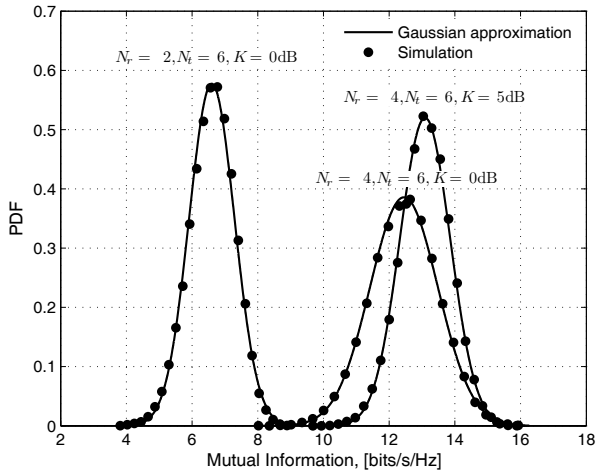

Fig. 4. Simulated MI PDF and Gaussian approximation for different model parameters ($\gamma = 10$ dB).

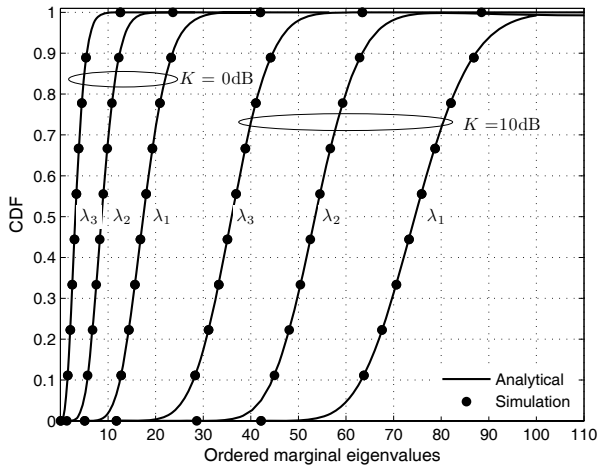

Fig. 5. Analytical and simulated marginal eigenvalue CDFs of a 3×8 LoS MIMO system.

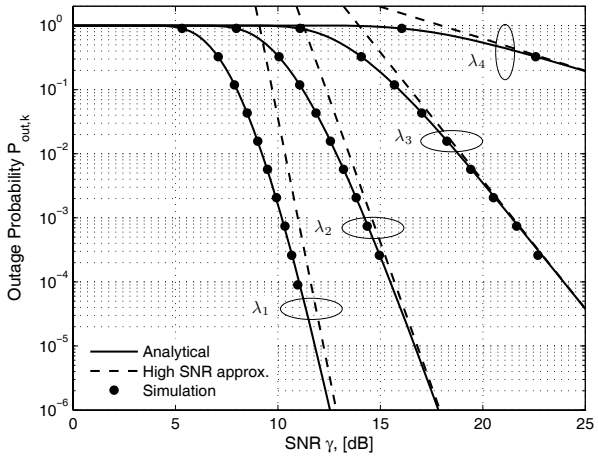

Fig. 6. Analytical, high-SNR approximation and simulated outage probability of a 4×4 LoS MIMO system against the SNR, γ ($K = 0$ dB and $\gamma_{\text{th}} = 10$ dB).

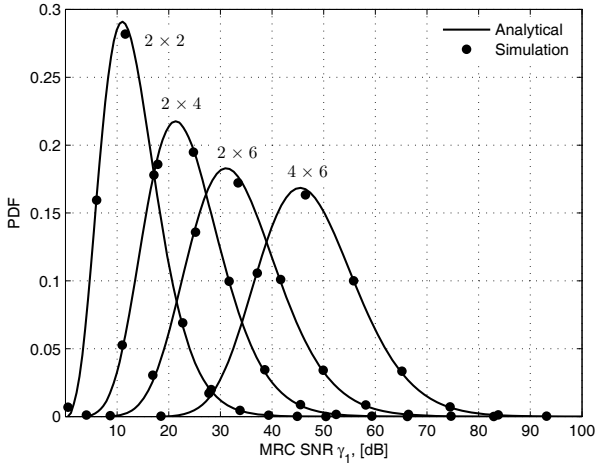

Fig. 7. Analytical and simulated output SNR PDF of different MIMO-MRC systems ($K = 0$ dB and $\gamma = 0$ dB).

outage probability against the SNR, γ, of a 4×4 MIMO system. The analytical and high-SNR approximation curves have been respectively generated via (56) and (57). The latter become exact even at moderate SNR values, while an increase in SNR pronounces the difference in outage between the first two dominant subchannels and the weakest ones. This important observation was also made in [25], and has motivated the design of efficient transmission schemes which adaptively allocate power to the active eigenmodes.

We finally consider a MIMO-MRC Rx, where only the dominant substream is used and $r = 1, p_1 = \gamma$. In Fig. 7, the output SNR PDF of MIMO-MRC is plotted for various antenna setups with the analytical curves being generated according to (59). By increasing the maximum number of antennas N_t, both the mean and spread of the SNR increase (enhanced diversity order) while an increase in N_r affects mainly the mean SNR (higher multiplexing gains). In Fig. 8, the outage is plotted versus the SNR for various antenna configurations with the same total number of antennas. As explicitly proved via (54), the optimal choice that asymptotically minimizes outage is to deploy symmetric MIMO systems with $N_t = N_r$.

VI. Conclusion

Optimized LoS MIMO configurations are of high practical importance for a plethora of emerging applications (e.g. indoor WLANs, peer-to-peer and vehicular communications) but, surprisingly, few publications have been reported on their statistical analysis. In fact, their capacity performance is the best achievable by any LoS MIMO configuration under UPA, which is the most meaningful transmission scheme when the Tx has no CSI. In this paper, our main goal has been to bridge this gap by providing a systematic capacity and MBF performance analysis. Using elements from random matrix theory, we have extended some recent results to the practically interesting case of orthogonal LoS subchannels, when the eigenvalues of the mean channel matrix become identical. In the first part of the paper, we have considered the first and second-order MI statistics for which novel exact and asymptotic high-SNR expressions were deduced. Our analytical results were further used to test the well-known Gaussianity approximation which was shown to hold under different simulation scenarios and low number of antennas.

In the second part of the paper, our focus was on the MBF

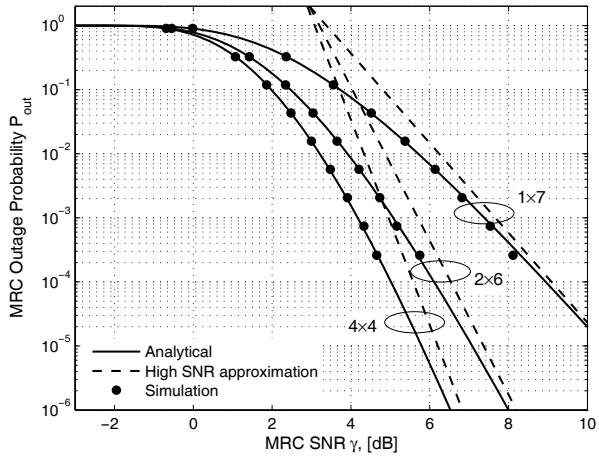

Fig. 8. Analytical, high-SNR approximation and simulated outage probability of a 4×4 LoS MIMO system against the SNR, γ.

performance assessment of these topologies via the channel eigenmodes. The exact marginal eigenvalue CDFs/PDFs along with their first-order expansions, around the origin, were derived and used to gain valuable insights into the SNR statistics (outage and PDF) of the associated MIMO eigenmodes. For the case of MRC receivers, where all power is allocated to the strongest eigenmode, it was demonstrated that the geometry of the Ricean paths has no impact on the asymptotic outage while the optimum choice in this context is to deploy the same number of transmit/receive antennas. As future work, the analytical knowledge of the eigenmode distributions can aid the design of adaptive algorithms, which systematically adapt the number of active eigenmodes, and thus achieve near-optimum performance with lower complexity.

APPENDIX A
PROOF OF THEOREM 1

The proof relies on the joint eigenvalue PDF for the case of distinct eigenvalues, which was originally given by James in [36] and manipulated into a more tractable form in [6]. In particular, we have

$$f(\boldsymbol{\lambda}) = \frac{\mathrm{etr}(-\boldsymbol{\omega})}{((t-s)!)^s |\boldsymbol{\Phi}(\boldsymbol{\omega})|} |\boldsymbol{\Psi}(\boldsymbol{\lambda})||\boldsymbol{\Phi}(\boldsymbol{\lambda})| \prod_{\ell=1}^{s} \lambda_\ell^{t-s} e^{-\lambda_\ell} \quad (60)$$

where $\{\boldsymbol{\Psi}(\boldsymbol{\lambda})\}_{i,j} = {}_0F_1(t-s+1;\lambda_i\omega_j)$, When the LoS eigenvalues coincide, (60) contains a term of the form

$$\lim_{\omega_1=\omega_2\ldots=\omega_s=\omega} \frac{|{}_0F_1(t-s+1;\lambda_i\omega_j)|}{|\boldsymbol{\Phi}(\boldsymbol{\omega})|} = \lim_{\omega_1=\omega_2\ldots=\omega_s=\omega} \frac{|{}_0F_1(t-s+1;\lambda_i\omega_j)|}{\prod_{i<j}^{s}(\omega_i-\omega_j)}. \quad (61)$$

To evaluate these determinant limits we employ the technique proposed in [30, Lemma 2]. Please note that a similar approach was adopted by Jin *et al.* in [25] as well, for the case of rank-L ($L \leq s$) non-centrality matrices with distinct eigenvalues. In particular, we successively apply the Cauchy's Mean Value Theorem and as such we take the $(s-j)$-th derivative across the j-th column, evaluated at $\omega_j = \omega$, or

$$\lim_{\omega_1=\omega_2\ldots=\omega_s=\omega} \frac{|\boldsymbol{\Psi}(\boldsymbol{\lambda})|}{|\boldsymbol{\Phi}(\boldsymbol{\omega})|} = \frac{\left|\frac{\mathrm{d}^{s-j}}{\mathrm{d}\omega^{s-j}} {}_0F_1(t-s+1;\lambda_i\omega)\right|}{\Gamma_s(s)} = \frac{((t-s)!)^s}{\Gamma_s(s)} \left| \sum_{k=0}^{\infty} \frac{\omega^k \lambda_i^{k+s-j}}{k!(t+k-j)!} \right|$$

where for the differentiation of ${}_0F_1(\alpha;x)$ we have used [39, Eq. (15.2.2)].

APPENDIX B
PROOFS OF HIGH-SNR EXPRESSIONS FOR THE MI STATISTICS

A. Proof of Lemma 1

The proof relies on [18, Eq. (22)], [16, Theorem 1] in which we consider the limiting case of identical LoS eigenvalues. To this end, we rewrite [16, Eq. (7)] according to

$$\begin{aligned}\phi(\upsilon) &= \lim_{\omega_1=\omega_2\ldots=\omega_s=\omega} \varepsilon^{2s\upsilon} \frac{\Gamma_s(t+\upsilon)\mathrm{etr}(-\boldsymbol{\omega})}{\Gamma_s(t)} \\ &\quad \times \frac{|{}_1F_1(t+\upsilon-s+j;t-s+j;\omega_i)\omega_i^{j-1}|}{\prod_{i<j}^{s}(\omega_j-\omega_i)} \\ &= \varepsilon^{2s\upsilon} \frac{\Gamma_s(t+\upsilon)\mathrm{etr}(-\boldsymbol{\omega})}{\Gamma_s(t)} \\ &\quad \times \lim_{\omega_1=\omega_2\ldots=\omega_s=\omega} \frac{|\mathbf{f}(\omega_1,\upsilon),\ldots,\mathbf{f}(\omega_s,\upsilon)|}{\prod_{i<j}^{s}(\omega_j-\omega_i)} \end{aligned} \quad (62)$$

where $\mathbf{f}(x,\upsilon) \triangleq [f_1(x,\upsilon),\ldots,f_s(x,\upsilon)]^T$ with $f_i(x,\upsilon) = {}_1F_1(t+\upsilon-s+i;t-s+i;x)x^{i-1}$. The above determinant limit is of the same form as (61) and thus we only need to compute the following derivative

$$\begin{aligned} f_i(\omega,\upsilon)^{(j-1)} &\triangleq \frac{\mathrm{d}^{(j-1)}}{\mathrm{d}\omega^{(j-1)}} f_i(\omega,\upsilon) \\ &= \frac{\mathrm{d}^{(j-1)}}{\mathrm{d}\omega^{(j-1)}} \sum_{k=0}^{\infty} \frac{(t+\upsilon-s+i)_k}{(t-s+i)_k} \frac{\omega^{k+i-1}}{k!} \end{aligned} \quad (63)$$

where $(\alpha)_n = \alpha(\alpha+1)\ldots(\alpha+n-1)$ is the Pochhammer symbol. We now consider two cases, these are $i<j$ or $i \geq j$. In the former case, (63) can be evaluated as

$$\begin{aligned} f_i(\omega,\upsilon)^{(j-1)} &= \sum_{k=j-i}^{\infty} \frac{(t+\upsilon-s+i+k-1)!}{(t+\upsilon-s+i-1)!} \\ &\times \frac{(t-s+i-1)!\omega^{k+i-j}}{k!(t-s+i+k-1)!}(k+i-1)\ldots(k+i-j+1) \\ &= \sum_{k=0}^{\infty} \frac{(t+\upsilon-s+j+k-1)!}{(t+\upsilon-s+i-1)!} \frac{(t-s+i-1)!}{(t-s+j+k-1)!} \\ &\times (k+j-1)\ldots(k+1)\frac{\omega^k}{(k+j-i)!} \\ &= \sum_{k=0}^{\infty} \frac{(t+\upsilon-s+j+k-1)!}{(t+\upsilon-s+i-1)!} \\ &\times \frac{(t-s+i-1)!}{(t-s+j+k-1)!} \frac{(k+j-1)!}{(k+j-i)!} \frac{\omega^k}{k!} \\ &= {}_2F_2(t+\upsilon-s+j,j;t-s+j,j-i+1;\omega) \\ &\times \frac{(t-s+i-1)!(t+\upsilon-s+j-1)!(j-1)!}{(t-s+j-1)!(t+\upsilon-s+i-1)!(j-i)!}. \end{aligned} \quad (64)$$

Applying the same procedure for $i \geq j$, we have

$$f_i(\omega,\upsilon)^{(j-1)} = \sum_{k=0}^{\infty} \frac{(t+\upsilon-s+i)_k}{(t-s+i)_k} \frac{(k+i-1)!}{(k+i-j)!} \frac{\omega^{k+i-j}}{k!}$$
$$= {}_2F_2(t+\upsilon-s+i, i; t-s+i, i-j+1; \omega) \frac{\omega^{i-j}(i-1)!}{(i-j)!} \tag{65}$$

and this concludes the proof.

B. Proof of Theorem 5

In the high-SNR regime (i.e. $\gamma \to \infty$), the MI expression in (8) is dominated by the second term, and as such

$$I^{\infty}(\mathbf{H}) = s \log_2\left(\frac{\gamma}{N_t}\right) + \frac{1}{\ln 2} \ln(\det(\mathbf{W})) \tag{66}$$

and thus for the mean MI it suffices to compute the term $\mathsf{E}\left[\ln(\det(\mathbf{W}))\right]$. The latter can be rewritten as

$$\mathsf{E}[\ln(|\mathbf{W}|)] = \left.\frac{\mathrm{d}\phi(\upsilon)}{\mathrm{d}\upsilon}\right|_{\upsilon=0} = \left.\frac{\mathrm{d}}{\mathrm{d}\upsilon} \ln \phi(\upsilon)\right|_{\upsilon=0} \tag{67}$$

where we have used that $\phi(0) = 1$ to obtain the last equality. Using (21) and omitting details, we obtain

$$\mathsf{E}[\ln(|\mathbf{W}|)] = \sum_{k=0}^{s-1} \psi(t-k) + s\ln(\varepsilon^2) + \frac{\frac{\mathrm{d}}{\mathrm{d}\upsilon}\det(\mathbf{A}(\upsilon))|_{\upsilon=0}}{|\mathbf{A}(0)|}. \tag{68}$$

For the evaluation of the above determinant at $\upsilon = 0$, we have

$$\frac{\mathrm{d}}{\mathrm{d}\upsilon}|\mathbf{A}(\upsilon)| = \sum_{\ell=1}^{s} \left|\mathbf{f}(\omega,\upsilon), \ldots, \frac{\mathrm{d}}{\mathrm{d}\upsilon}\left[\mathbf{f}(\omega,\upsilon)^{(\ell-1)}\right], \ldots, \mathbf{f}(\omega,\upsilon)^{(s-1)}\right| \tag{69}$$

where we have introduced the compact notation for the derivative wrt to ω, $\mathbf{f}(\omega,\upsilon)^{(j-1)} = \frac{\mathrm{d}^{(j-1)}}{\mathrm{d}\omega^{(j-1)}}\mathbf{f}(\omega,\upsilon)$. In order to compute the required derivatives, we consider two cases as in Appendix B-A according to the values of the indices i and j. In particular, for $i \geq j$, we use (65) to get

$$\frac{\mathrm{d}}{\mathrm{d}\upsilon}\left[f_i(\omega,\upsilon)^{(j-1)}\right] = \sum_{k=0}^{\infty} \frac{1}{(t-s+i)_k} \frac{(k+i-1)!}{(k+i-j)!} \frac{\omega^{k+i-j}}{k!} \times \frac{\mathrm{d}}{\mathrm{d}\upsilon}(t+\upsilon-s+i)_k \tag{70}$$

and

$$\frac{\mathrm{d}}{\mathrm{d}\upsilon}(t+\upsilon-s+i)_k$$
$$= \frac{\mathrm{d}}{\mathrm{d}\upsilon}(t+\upsilon-s+i+k-1)\ldots(t+\upsilon-s+i)$$
$$= (t+\upsilon-s+i+k-1)\ldots(t+\upsilon-s+i) \times \left(\sum_{n=0}^{k-1} \frac{1}{t+\upsilon-s+i+n}\right)$$
$$= (t+\upsilon-s+i)_k \left(\sum_{n=0}^{k-1} \frac{1}{t+\upsilon-s+i+n}\right). \tag{71}$$

Substituting (71) into (70), removing the vanishing $k=0$ term and setting $\upsilon = 0$, we get the desired result. Likewise, for $i < j$, we use (64) to express the required derivative as

$$\frac{\mathrm{d}}{\mathrm{d}\upsilon}\left[f_i(\omega,\upsilon)^{(j-1)}\right] = \sum_{k=0}^{\infty} \frac{(t-s+i-1)!}{(t-s+j+k-1)!} \frac{(k+i-1)!}{(k+j-i)!} \frac{\omega^k}{k!} \times \frac{\mathrm{d}}{\mathrm{d}\upsilon}\left(\frac{(t+\upsilon-s+j+k-1)!}{(t+\upsilon-s+i-1)!}\right). \tag{72}$$

Using the same methodology as above and some basic algebraic manipulations we conclude the proof.

C. Proof of Theorem 6

In the high-SNR regime (i.e. $\gamma \to \infty$), the MI variance becomes

$$\mathsf{Var}\left[I^{\infty}(\mathbf{H})\right] = \mathsf{Var}\left[\log_2 \det\left(\frac{\gamma}{N_t}\mathbf{H}\mathbf{H}^{\dagger}\right)\right] = \frac{1}{(\ln 2)^2}\mathsf{Var}\left[\ln(\det(\mathbf{W})\right]. \tag{73}$$

Using [16, Eq. (165)], we can express the variance remaining term in (73)

$$\mathsf{Var}\left[\ln(\det(\mathbf{W})\right] = \left.\frac{\mathrm{d}^2}{\mathrm{d}\upsilon^2}\ln(\phi(\upsilon))\right|_{\upsilon=0} = \sum_{k=0}^{s-1}\psi'(t-k) + \frac{\frac{\mathrm{d}^2}{\mathrm{d}\upsilon^2}\det(\mathbf{A}(\upsilon))|_{\upsilon=0}}{|\mathbf{A}(0)|} - \left(\frac{\frac{\mathrm{d}}{\mathrm{d}\upsilon}\det(\mathbf{A}(\upsilon))|_{\upsilon=0}}{|\mathbf{A}(0)|}\right)^2 \tag{74}$$

where the second line follows from differentiation of (68). In order to compute the second derivative term in (74), we consider the case $i \geq j$ which via (70)–(71) results in

$$\frac{\mathrm{d}^2}{\mathrm{d}\upsilon^2}\left[f_i(\omega,\upsilon)^{(j-1)}\right] = \sum_{k=1}^{\infty} \frac{1}{(t-s+i)_k} \frac{(k+i-1)!}{(k+i-j)!} \frac{\omega^{k+i-j}}{k!} \times \frac{\mathrm{d}}{\mathrm{d}\upsilon}\left((t+\upsilon-s+i)_k \left(\textstyle\sum_{n=0}^{k-1} \frac{1}{t+\upsilon-s+i+n}\right)\right). \tag{75}$$

Then, it is easy to see that

$$\frac{\mathrm{d}}{\mathrm{d}\upsilon}\left((t+\upsilon-s+i)_k\left(\sum_{n=0}^{k-1}\frac{1}{t+\upsilon-s+i+n}\right)\right)$$
$$= (t+\upsilon-s+i)_k\left(\left(\sum_{n=0}^{k-1}\frac{1}{t+\upsilon-s+i+n}\right)^2 - \sum_{n=0}^{k-1}\frac{1}{(t+\upsilon-s+i+n)^2}\right)$$
$$= (t+\upsilon-s+i)_k \times \left(\sum_{n=0}^{k-2}\sum_{m=n+1}^{k-1}\frac{2}{(t+\upsilon-s+i+n)(t+\upsilon-s+i+m)}\right). \tag{76}$$

Substituting (76) into (75), setting $\upsilon = 0$ and following the same process for $i < j$, we can obtain the final result after combining (74) with (69)–(72) and factorization.

Appendix C
Proof of Theorem 11

In order to compute the first-order approximation of $\sum_1 |\mathbf{\Omega}(x)|$ in (44), we have to apply a Taylor expansion

around the origin on the elements of $\mathbf{\Omega}(x)$ in (45). For any matrix $\mathbf{\Upsilon}(x)$, the Taylor expansion reads as

$$\{\mathbf{\Upsilon}(x)\}_{i,j} = \sum_{p=0}^{n} \left\{\mathbf{\Upsilon}^{(p)}(0)\right\}_{i,j} \frac{x^p}{p!} + o(x^n). \tag{77}$$

We now introduce the infinite polynomial representations of both incomplete gamma functions in (36) and (41). For the latter case, we have

$$\{\mathbf{\Xi}(x)\}_{i,j} = \sum_{k=0}^{\infty} \frac{\omega^k e^{-x}(t+k+s-i-j)!}{k!(t+k-j)!} \times \left(\sum_{p=t+k+s-i-j+1}^{\infty} \frac{x^p}{p!}\right) \tag{78}$$

$$= \sum_{k=0}^{\infty} \frac{\omega^k (t+k+s-i-j)!}{k!(t+k-j)!} \times \left(\sum_{n=0}^{\infty}\sum_{p=0}^{\infty} \frac{(-1)^n x^{p+n+t+k+s-i-j+1}}{n!(p+t+k+s-i-j+1)!}\right) \tag{79}$$

where from (78) to (79), we have expanded the exponential function as an infinite series and then factorized. In order to compute the first-order expansion of $\{\mathbf{\Xi}(x)\}_{i,j}$, we have to consider only the first non-vanishing term in (77). From (79), it is clear that the first $(t+s-i-j)$-th derivatives are equal to zero when $x = 0$. Thus, we only need to compute the $(t+s-i-j+1)$-th derivative and evaluate it at zero:

$$\{\mathbf{\Xi}(x)\}_{i,j}^{(t+s-i-j+1)} = \sum_{k=0}^{\infty} \frac{\omega^k (t+k+s-i-j)!}{k!(t+k-j)!} \times \left(\sum_{n=0}^{\infty}\sum_{p=0}^{\infty} \frac{(-1)^n (p+n+t+k+s-i-j+1)! x^{p+n+k}}{(p+n+k)!n!(p+t+k+s-i-j+1)!}\right)$$

$$\{\mathbf{\Xi}(x\}_{i,j}^{(t+s-i-j+1)}\Big|_{x=0} = \frac{(t+s-i-j)!}{(t-j)!}. \tag{80}$$

Combining (80) with (77), we get the dominant non-vanishing term of the Taylor expansion

$$\{\mathbf{\Xi}(x)\}_{i,j} = \frac{x^{t+s-i-j+1}}{(t-j)!(t+s-i-j+1)} + o(x^{t+s-i-j+1}). \tag{81}$$

Following a similar procedure for $\{\mathbf{\Theta}(x)\}_{i,j}$, the first-order expansion of each element of $\mathbf{\Omega}(x)$ becomes as in (82) at the top of next page. From (82), it is clear that only the second matrix branch depends on x, and since $\alpha_i > 0$ is combined with a negative sign, the values taken by $(\alpha_1, \ldots, \alpha_s)$ over $\{k, \ldots, s\}$ should be maximum, i.e., equal to $\{k, \ldots, s\}$. From the definition of the summation $\sum_1$ in (44), it follows that there will be only one determinant with the smallest exponent in x, denoted as $|\mathbf{\Delta}_{\text{id}}|$, which corresponds to the identity permutation $(\alpha_1, \alpha_2, \ldots, \alpha_s) = (1, 2, \ldots, s)$. This determinant, $|\mathbf{\Delta}_{\text{id}}|$, after factorization and after dropping the $o(\cdot)$ term for the sake of brevity, becomes

$$|\mathbf{\Delta}_{\text{id}}| = \frac{x^{(t-k+1)(s-k+1)-(s-k+1)(k-1)-\frac{(s-k+1)(s-k)}{2}}}{\Gamma_s(t)} |\mathbf{\Delta}(x)| \tag{83}$$

with $\mathbf{\Delta}(x)$ is defined in (84) on the top of next page. We can now rewrite $|\mathbf{\Delta}(x)|$ using the Leibniz definition for a matrix determinant as follows

$$|\mathbf{\Delta}(x)| = \sum_{\sigma} \text{sgn}(\sigma) \prod_{i=1}^{s} \{\mathbf{\Delta}(x)\}_{i,\sigma_i} \tag{85}$$

where $\sigma = (\sigma_1, \ldots, \sigma_s)$ is a permutation of $\{1, \ldots, s\}$. Using (84), we can get

$$\prod_{i=1}^{s} \{\mathbf{\Delta}(x)\}_{i,\sigma_i} = \prod_{i=1}^{k-1} (t+s-i-\sigma_i)!\, {}_1F_1(t+s-i-\sigma_i+1; t-\sigma_i+1; \omega) \times \prod_{i=k}^{s} \frac{x^{s+1-\sigma_i}}{t+s-i-\sigma_i+1}. \tag{86}$$

In order to obtain the elements with the smallest exponent in x, we need to keep only the permutations maximizing $\sum_{i=k}^{s} \sigma_i$, and hence the unordered subset $\{\sigma_k, \ldots, \sigma_s\}$ should be equal to $\{k, \ldots, s\}$. Thus, the permutation σ can be split into two permutations $a = (a_1, \ldots, a_{k-1})$ of $\{1, \ldots, k-1\}$ and $b = (b_k, \ldots, b_s)$ of $\{k, \ldots, s\}$ and as such the determinant in (83) can be rewritten as

$$|\mathbf{\Delta}(x)| = \sum_{a} \text{sgn}(a) \prod_{i=1}^{k-1} \{\mathbf{\Delta}(x)\}_{i,a_i} \times \sum_{b} \text{sgn}(b) \prod_{i=k}^{s} \{\mathbf{\Delta}(x)\}_{i,b_i} \tag{87}$$

which after some basic algebra and factorization of x becomes

$$|\mathbf{\Delta}(x)| = x^{(s-k+1)(k-1)+\frac{(s-k+1)(s-k)}{2}} |\mathbf{\Delta}_1||\mathbf{\Delta}_2|. \tag{88}$$

Substituting (88) in (83) yields the Taylor expansion of $\sum_1 |\mathbf{\Omega}(x)|$, which scales as $x^{(t-k+1)(s-k+1)}$. The proof concludes after observing that the $(k-1)$-th eigenvalue in (44) scales with a larger exponent and thus can be neglected. The PDF expression (51) follows by differentiating (50) wrt x.

ACKNOWLEDGMENTS

The authors would like to thank the Associate Editor as well as the anonymous reviewers for their constructive comments which helped to improve the quality of this manuscript.

REFERENCES

[1] I. E. Telatar, "Capacity of multi-antenna Gaussian channels," *Europ. Trans. Telecommun.*, vol. 10, no. 6, pp. 585–595, Nov./Dec. 1999.

[2] M. Chiani, M. Z. Win, and A. Zanella, "On the capacity of spatially correlated MIMO Rayleigh-fading channels," *IEEE Trans. Inf. Theory*, vol. 49, no. 10, pp. 2363–2371, Oct. 2003.

[3] A. Grant, "Rayleigh fading multi-antenna channels," *EURASIP J. Appl. Signal Process.*, vol. 2002, no. 3, pp. 316–329, Mar. 2002.

[4] H. Shin and J. H. Lee, "Capacity of multi-antenna fading channels: spatial fading correlation, double scattering, and keyhole," *IEEE Trans. Inf. Theory*, vol. 49, no. 10, pp. 2636–2647, Oct. 2003.

[5] Ö. Oyman, R. U. Nabar, H. Bölcskei, and A. J. Paulraj, "Characterizing the statistical properties of mutual information in MIMO channels," *IEEE Trans. Signal Process.*, vol. 51, no. 11, pp. 2784–2795, Nov. 2003.

[6] M. Kang and M.-S. Alouini, "Capacity of MIMO Rician channels," *IEEE Trans. Wireless Commun.*, vol. 5, no. 1, pp. 112–122, Jan. 2006.

[7] J. Hansen and H. Bölcskei, "A geometrical investigation of the rank-1 Rician MIMO channel at high SNR," in *Proc. IEEE Int. Symp. Inf. Theory (ISIT)*, July 2004, p. 64.

$$\{\mathbf{\Omega}(x)\}_{\alpha_i,j} = \begin{cases} \frac{(t+s-\alpha_i-j)!}{(t-j)!}{}_1F_1(t+s-\alpha_i-j+1;t-j+1;\omega)+o(1), & i=1,\ldots,k-1 \\ \frac{x^{t+s-\alpha_i-j+1}}{(t-j)!(t+s-\alpha_i-j+1)}+o(x^{t+s-\alpha_i-j+1}), & i=k,\ldots,s. \end{cases} \tag{82}$$

$$\{\mathbf{\Delta}(x)\}_{i,j} = \begin{cases} (t+s-i-j)!{}_1F_1(t+s-i-j+1;t-j+1;\omega), & i=1,\ldots,k-1 \\ x^{s+1-j}/(t+s-i-j+1), & i=k,\ldots,s. \end{cases} \tag{84}$$

[8] S. Jin, X. Gao, and X. You, "On the ergodic capacity of rank-1 Ricean-fading MIMO channels," *IEEE Trans. Inf. Theory*, vol. 53, no. 2, pp. 502–517, Feb. 2007.

[9] F. Bøhagen, P. Orten, and G. E. Øien, "Construction and capacity analysis of high-rank line-of-sight MIMO channels," in *Proc. IEEE Wireless Commun. Networking Conf. (WCNC)*, Mar. 2005, pp. 432–437.

[10] —, "Design of capacity-optimal high-rank line-of-sight MIMO channels," *IEEE Trans. Wireless Commun.*, vol. 6, no. 4, pp. 1420–1425, Apr. 2007.

[11] I. Sarris and A. R. Nix, "Design and performance assessment of high-capacity MIMO architectures in the presence of a line-of-sight component," *IEEE Trans. Veh. Technol.*, vol. 56, no. 4, pp. 2194–2202, July 2007.

[12] M. Matthaiou, D. I. Laurenson, and C. -X. Wang, "Capacity study of vehicle-to-roadside MIMO channels with a line-of-sight component," in *Proc. IEEE Wireless Commun. Networking Conf. (WCNC)*, Mar. 2008, pp. 775–779.

[13] M. Matthaiou, A. Pitarokoilis, and J. A. Nossek, "Mutual information statistics of optimized LoS MIMO configurations," in *Proc. IEEE Int. Conf. Commun. (ICC)*, May 2010.

[14] S. K. Jayaweera and H. V. Poor, "On the capacity of multiple-antenna systems in Ricean fading," *IEEE Trans. Wireless Commun.*, vol. 4, no. 3, pp. 1102–1111, Mar. 2005.

[15] A. Maaref and S. Aïssa, "Joint and marginal eigenvalue distributions of (non)central complex Wishart matrices and PDF-based approach for characterizing the capacity statistics of MIMO Ricean and Rayleigh fading channels," *IEEE Trans. Wireless Commun.*, vol. 6, no. 10, pp. 3607–3619, Oct. 2007.

[16] M. R. McKay and I. B. Collings, "General capacity bounds for spatially correlated Rician MIMO channels," *IEEE Trans. Inf. Theory*, vol. 51, no. 9, pp. 3121–3145, Sep. 2005.

[17] —, "On the capacity of frequency-flat and frequency-selective Rician MIMO channels with single-sided correlation," *IEEE Trans. Wireless Commun.*, vol. 5, no. 8, pp. 2038–2043, Aug. 2005.

[18] X. W. Cui, Q. T. Zhang, and Z. M. Feng, "Generic procedure for tightly bounding the capacity of MIMO correlated Rician fading channels," *IEEE Trans. Commun.*, vol. 53, no. 5, pp. 890–898, May 2005.

[19] M. Matthaiou, Y. Kopsinis, D. I. Laurenson, and A. M. Sayeed, "Upper bound for the ergodic capacity of dual MIMO Rician systems: simplified derivation and asymptotic tightness," *IEEE Trans. Commun.*, vol. 57, no. 12, pp. 3589–3596, Dec. 2009.

[20] Y. Zhu, P.-Y. Kam, and Y. Xin, "On the mutual information distribution of MIMO Rician fading channels," *IEEE Trans. Commun.*, vol. 57, no. 15, pp. 1453–1462, May 2009.

[21] G. Taricco, "Asymptotic mutual information statistics of separately correlated Rician fading MIMO channels," *IEEE Trans. Inf. Theory*, vol. 54, no. 9, pp. 3490–3504, Aug. 2008.

[22] D. P. Palomar, J. M. Cioffi, and M. A. Lagunas, "Joint Tx-Rx beamforming design for multicarrier MIMO channels: a unified framework for convex optimization," *IEEE Trans. Signal Process.*, vol. 51, no. 9, pp. 2381–2401, Sep. 2003.

[23] L. G. Ordõnez, D. P. Palomar, A. Pagès Zamora, and J. R. Fonollosa, "High-SNR analytical performance of spatial multiplexing MIMO systems with CSI," *IEEE Trans. Signal Process.*, vol. 55, no. 11, pp. 5447–5463, Nov. 2007.

[24] L. G. Ordóñez, D. P. Palomar, and J. R. Fonollosa, "Ordered eigenvalues of a general class of Hermitian random matrices with application to the performance analysis of MIMO systems," *IEEE Trans. Signal Process.*, vol. 57, no. 2, pp. 672–689, Feb. 2009.

[25] S. Jin, M. R. McKay, X. Gao, and I. B. Collings, "MIMO multichannel beamforming: SER and outage using new eigenvalue distribution of complex noncentral Wishart matrices," *IEEE Trans. Commun.*, vol. 56, no. 3, pp. 424–434, Mar. 2008.

[26] A. Zanella, M. Chiani, and M. Z. Win, "On the marginal distribution of the eigenvalues of Wishart matrices," *IEEE Trans. Commun.*, vol. 57, no. 4, pp. 1050–1060, Apr. 2009.

[27] M. Chiani and A. Zanella, "Joint distribution of an arbitrary subset of the ordered eigenvalues of Wishart matrices," in *Proc. IEEE Pers. Indoor Mobile Radio Conf. (PIMRC)*, Sep. 2008.

[28] A. Zanella and M. Chiani, "The PDF of the lth largest eigenvalue of central Wishart matrices and its application to the performance analysis of MIMO systems," in *Proc. IEEE Global Telecommun. Conf. (GLOBECOM)*, Nov. 2008, pp. 201–206.

[29] F. Bøhagen, P. Orten, G. E. Øien, and S. de la Kethulle de Ryhove, "Exact capacity expressions for dual-branch Ricean MIMO systems," *IEEE Trans. Commun.*, vol. 56, no. 12, pp. 2214–2222, Dec. 2008.

[30] M. Chiani, M. Z. Win, and H. Shin, "MIMO networks: the effects of interference," *IEEE Trans. Inf. Theory*, vol. 56, no. 1, pp. 336–349, Jan. 2010.

[31] F. Rashid-Farrokhi, A. Lozano, G. J. Foschini, and R. A. Valenzuela, "Spectral efficiency of wireless systems with multiple transmit and receive antennas," in *Proc. IEEE Int. Symp. Pers. Indoor Mobile Radio Commun. (PIMRC)*, Sep. 2000, vol. 1, pp. 373–377.

[32] V. Erceg, *et al.*, "TGn channel models," IEEE 802.11-03/940r4. [Online]. Available: http://www.802wirelessworld.com:8802

[33] I. Sarris and A. R. Nix, "Rician K-factor measurements in a home and an office environment in the 60 GHz band," in *Proc. IST Mob. Wireless Commun. Summit*, July 2007.

[34] A. Paier, *et al.*, "Characterization of vehicle-to-vehicle radio channels from measurements at 5.2 GHz," *Wireless Personal Commun.*, vol. 6, June 2008.

[35] J. Wishart, "The generalized product moment distribution in samples from a normal multivariate population," *Biometrica*, vol. 20A, pp. 32–52, 1928.

[36] A. T. James, "Distributions of matrix variates and latent roots derived from normal samples," *Ann. Math. Stat.*, vol. 35, no. 2, pp. 475–501, June 1964.

[37] I. S. Gradshteyn and I. M. Ryzhik, *Table of Integrals, Series, and Products*, 7th edition. San Diego, CA: Academic Press, 2007.

[38] A. M. Tulino, A. Lozano, and S. Verdú, "Capacity-achieving input covariance for single-user multiantenna channels," *IEEE Trans. Wireless Commun.*, vol. 5, no. 2, pp. 662–671, Mar. 2006.

[39] M. Abramowitz and I. A. Stegun, *Handbook of Mathematical Functions with Formulas, Graphs, and Mathematical Tables*, 9th edition. New York: Dover, 1970.

[40] D. Williams, *Probability with Martingales (Cambridge Mathematical Textbooks)*. Cambridge University Press, 2001.

[41] J. Chen and K.-K. Wong, "Power minimization of central Wishart MIMO block-fading channels," *IEEE Trans. Commun.*, vol. 57, no. 4, pp. 899–905, Apr. 2009.

[42] P. J. Smith and M. Shafi, "On a Gaussian approximation to the capacity of wireless MIMO systems," in *Proc. IEEE Int. Conf. Commun. (ICC)*, Apr. 2002, pp. 406–410.

[43] M. Kang and M.-S. Alouini, "Largest eigenvalue of complex Wishart matrices and performance analysis of MIMO MRC systems," *IEEE J. Sel. Areas Commun.*, vol. 21, no. 3, pp. 418–426, Apr. 2003.

[44] P. R. Dighe, R. K. Mallik, and S. S. Jamuar, "Analysis of transmit-receive diversity in Rayleigh fading," *IEEE Trans. Commun.*, vol. 51, no. 4, pp. 694–703, Apr. 2003.

[45] A. Zanella, M. Chiani, and M. Z. Win, "Performance of MIMO MRC in correlated Rayleigh fading environments," in *Proc. IEEE Veh. Technol. Conf. (VTC)*, May 2005, pp. 1633–1637.

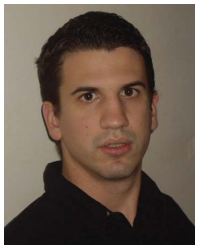

Michail Matthaiou (S'05-M'08) was born in Thessaloniki, Greece in 1981. He obtained the Diploma degree (five years) in electrical and computer engineering from the Aristotle University of Thessaloniki, Greece in 2004. He then received the M.Sc. (with distinction) in communication systems and signal processing from the University of Bristol, U.K. and Ph.D. degrees from the University of Edinburgh, U.K. in 2005 and 2008, respectively. From September 2008 through May 2010, he was with the Institute for Circuit Theory and Signal Processing, Munich University of Technology (TUM), Germany working as a Postdoctoral Research Associate. In June 2010, he joined Chalmers University of Technology, Gothenburg, Sweden as an Assistant Professor. His research interests span signal processing for wireless communications, random matrix theory for MIMO systems, multivariate statistics, and performance analysis of fading channels. Dr. Matthaiou is a co-recipient of the 2006 IEEE Communications Chapter Project Prize for the best M.Sc. dissertation in the area of communications.

Paul de Kerret (S'10) was born in 1987 in Paris, France. In 2009, he graduated from the Ecole Nationale Supérieure des Télécommunications de Bretagne, France and obtained a diploma degree in electrical engineering from Munich University of Technology (TUM), Germany. He also earned a four year degree in mathematics at the Université de Bretagne Occidentale, France in 2008. Since January 2010, he has been a research assistant at the Institute for Theoretical Information Technology, RWTH Aachen University, Germany. His research mainly focuses on transmission in multiple antenna systems and includes precoder optimization, random matrix theory, multiuser transmission, and MIMO networks.

George K. Karagiannidis (M'97-SM'04) was born in Pithagorion, Samos Island, Greece. He received the University Diploma (5 years) and Ph.D degree, both in electrical and computer engineering, from the University of Patras, in 1987 and 1999, respectively. From 2000 to 2004, he was a Senior Researcher at the Institute for Space Applications and Remote Sensing, National Observatory of Athens, Greece. In June 2004, he joined Aristotle University of Thessaloniki, Thessaloniki, where he is currently an Associate Professor of Digital Communications Systems in the Electrical and Computer Engineering Department and Head of the Telecommunications Systems and Networks Lab.

Dr. Karagiannidis has been a member of Technical Program Committees for several IEEE conferences such as ICC, GLOBECOM, etc. He is a member of the editorial board of the IEEE TRANSACTIONS ON COMMUNICATIONS, Senior Editor of IEEE COMMUNICATIONS LETTERS and Lead Guest Editor of the special issue on "Optical Wireless Communications" of the IEEE JOURNAL ON SELECTED AREAS ON COMMUNICATIONS. He is co-recipient of the Best Paper Award of the Wireless Communications Symposium (WCS) in the IEEE International Conference on Communications (ICC'07), Glasgow, U.K., June 2007. Dr. Karagiannidis is the Chair of the IEEE COMSOC Greek Chapter.

Josef A. Nossek (S'72-M'74-SM'81-F'93) received the Dipl.-Ing. and the Dr. techn. degrees in electrical engineering from the University of Technology in Vienna, Austria in 1974 and 1980, respectively. In 1974 he joined Siemens AG in Munich, Germany as a member of technical staff, in 1978 he became supervisor, and from 1980 on he was Head of Department. In 1987 he was promoted to Head of all radio systems design. Since 1989, he has been a Full Professor of circuit theory and signal processing at the Munich University of Technology, where he teaches undergraduate and graduate courses on circuit and systems theory and signal processing, and leads research on signal processing algorithms for communications. He was President Elect, President, and Past President of the IEEE Circuits and Systems Society in 2001, 2002 and 2003 respectively. He was Vice President of VDE (Verband der Elektrotechnik, Elektronik und Informationstechnik e.V.) in 2005 and 2006, President of VDE 2007 and 2008, and was again Vice President of VDE in 2009 and 2010. His awards include the ITG Best Paper Award (1988), the Mannesmann Mobilfunk (now Vodafone) Innovations Award (1998), the Award for Excellence in Teaching from the Bavarian Ministry for Science, Research and Art in 1998, and the Golden Jubilee Medal of the IEEE Circuits and Systems Society for "Outstanding Contributions to the Society" in 1999. In 2008 he received the Education Award of the IEEE Circuits and Systems Society and the Order of Merit from the the Federal Republic of Germany. Since 2009 he has been a Member of the National Academy of Engineering Sciences of Germany (acatech).